



Assessment of sugar cane straw ash (SCSA) as pozzolanic material in blended Portland cement: Microstructural characterization of pastes and mechanical strength of mortars



J.C.B. Moraes^a, J.L. Akasaki^a, J.L.P. Melges^a, J. Monzó^b, M.V. Borrachero^b, L. Soriano^b, J. Payá^b, M.M. Tashima^{a,*}

^aUNESP – Univ Estadual Paulista, Campus de Ilha Solteira, São Paulo, Brazil

^bICITECH – Instituto de Ciencia y Tecnología del Hormigón, Universitat Politècnica de València, Valencia, Spain

HIGHLIGHTS

- Highly pozzolanic sugar cane straw ash (SCSA) was obtained by means auto-combustion.
- SCSA fixed present Ca(OH)₂ in 3/7 hydrated lime/SCSA systems after 3 days at 20 °C.
- The pozzolanic reaction in OPC/SCSA systems took place in the 1–90 days period.
- Blended SCSA–OPC mortars in the range 15–30% yielded similar strength than control.
- SCSA presented excellent characteristics for producing high quality OPC-based binders.

ARTICLE INFO

Article history:

Received 11 February 2015

Received in revised form 16 June 2015

Accepted 14 July 2015

Available online 18 July 2015

Keywords:

Sugar cane straw ash

Auto-combustion

Portland cement

Microstructural characterization

Mechanical properties

Pozzolanic reactivity

Lime paste

Cement paste

Mortar

ABSTRACT

The aim of this paper is to assess the pozzolanic reactivity of sugar cane straw ash (SCSA) obtained through an auto-combustion process and the mechanical properties of SCSA-containing systems. Characterization of SCSA (X-ray diffraction, chemical composition, particle size, and microscopy) and reactivity studies on hydrated lime/SCSA and Portland cement/SCSA pastes through infrared spectroscopy, thermogravimetric analysis, and microscopy demonstrated the high pozzolanic activity. This reactivity made it possible to achieve good mechanical properties in mortars in which 15–30% of the cement was replaced by SCSA. After 90 days of curing, the SCSA fixed 100% of the lime present in lime/SCSA pastes, and the compressive strength of mortars containing SCSA reached 44 MPa, a value similar to those found for control mortars after the same number of curing days. The results for the microstructural and mechanical properties showed that SCSA is a good pozzolanic material.

© 2015 Elsevier Ltd. All rights reserved.

1. Introduction

Portland cement is widely used in the world nowadays, with a global consumption about of 3.7 billion tons [1]. In addition, Portland cement production represents 5–8% of total CO₂ emissions in the world [2], and to produce 1 ton of the binder, 2.8 tons of raw materials are necessary [3]. This information shows how important it is to reduce consumption of Portland cement due the environmental problems caused by its production. Hence, to

reduce these problems, alternative materials are being researched, and one of the solutions is to use pozzolanic materials to partially replace the Portland cement.

Pozzolanic materials were first used in the Roman Empire, when natural pozzolans were mixed with lime to create a strong and durable material for civil buildings [4–6]. Nowadays, pozzolans are used not only for ecological reasons but also for technological ones, because this material increases the mechanical strength and improves the durability of blended Portland cements [5–17]. There are two main types of pozzolanic materials: natural and artificial. Natural pozzolans are related to the residues from volcanic activities or deposits of diatomaceous earth, whereas

* Corresponding author.

E-mail address: maumitta@hotmail.com (M.M. Tashima).

artificial pozzolans are related to products (e.g. metakaolin) and byproducts or waste from industry and agro-industry [4].

Examples of byproducts from industry that are widely known as pozzolanic materials are silica fume and fly ash [18–20]. Many byproducts made from commodity crops are cheap, plentiful, globally distributed, and renewable resources that are suitable for the production of pozzolans: rice husks, sugar cane bagasse, palm oil wastes, wheat straw, eucalyptus waste, and bamboo leaves, among others [21,22]. In this way, these agro-industry wastes can be converted into ashes (with or without energy recovery), and researches on them are being conducted due to the good results obtained when using them to partially replace Portland cement [21–27]. In this context, this paper presents another agro-industry waste from sugar cane production: sugar cane straw ash (SCSA).

The problem related to SCSA starts with the production of sugar cane, which is increasing in Brazil due the production of sugar, alcohol, and energy. In 2003/2004, sugar cane production in Brazil was 358.7 million tons and, in 2013/2014, it expanded to 653.4 million tons [28], which represents an increment of 82.2% in the production of sugar cane in only 10 years. The part of the plant that is removed during the sugar cane collection is called sugar cane straw, and it is composed of leaves and the top of the plant [29]. According to the Center of Strategic Studies Management (CGEE), 1000 kg of sugar cane generates 140 kg of sugar cane straw [30]. Since this byproduct is mostly left in the field after the harvest, there are researches on new techniques to collect the sugar cane straw in order to generate energy [31]. The calorific value of sugar cane straw is in the range of 13–19 kJ/ton [31–33] and can be compared to the sugar cane bagasse [34], becoming attractive to generate energy through a burning process.

After burning of the sugar cane straw, a waste is generated: the SCSA. Studies showed that around 3–5.5 kg of ash is obtained from burning 100 kg of sugar cane straw [33,35]. Knowing the problems of disposal and the high volume of the residue, an appropriate final destination for this ash would be the building construction sector as a pozzolanic material, which partially replaces the Portland cement.

Some authors previously studied the pozzolanic activity of SCSA and highlighted that it is a very reactive pozzolan [35–40]. Comparisons between SCSA and other pozzolanic materials from the agro-industry have been carried out. Martirena et al. [36] compared SCSA and sugar cane bagasse ash (SCBA) in hydrated lime–pozzolan pastes. Through microstructural analysis, the authors concluded that SCSA is more reactive than SCBA at earlier curing times and that mortars containing SCSA presented higher compressive strength after 28 days of curing. In addition, Villar-Cociña et al. compared SCSA and rice husk ash (RHA) by a kinetic-diffusive model to evaluate their reactivity. In this comparison, the authors established that SCSA presented better reactivity [37].

It is well known that the temperature of calcination influences the pozzolanic properties of ashes. Thus, some authors studied different preparations of SCSA. Martirena et al. [38] studied a rudimentary incinerator for burning straw to obtain SCSA and compared it to straw burnt in the open air. The burning temperature in the incinerator was 600 °C for 1–3 h, and the remaining ash was cooled for 2 h. From thermogravimetric analysis (TGA), X-ray diffraction (XRD), scanning electron microscopy (SEM), and the compressive strength of pastes, it was concluded that there are no significant differences between open air and incinerator burning, due the long time in the incinerator and the slow cooling process. Frías et al. [35] studied two different temperatures of straw calcination during 20 min: 800 and 1000 °C. Both SCSAs obtained were characterized and assessed through lime fixation, and the authors concluded that both ashes presented similar

activity. Guzmán et al. [40] assessed three procedures to obtain SCSA: burning at 590 and 700 °C and a combined method with pre-combustion and burning at 700 °C. The third method presented the highest amorphous silica content, and the corresponding ash in mortars that replaced partially the Portland cement was assessed. The authors concluded that the best content of SCSA in terms of mechanical development was between 10% and 20% substitution. Additional research was carried out on the preparation of pozzolans by calcination of a mixture of sugar cane straw and clay (20–30%): SCSA had a high pozzolanic activity but its reactivity decreased with increasing clay content and calcination temperature [41].

This interesting field of reusing agro-wastes in the production of binders requires more research related to the reactivity and microstructure of SCSA-containing binders. Moreover, easier methods of obtaining SCSA are necessary in order to have sufficient amounts for preparing different types of mixtures. In this work, the main objective is to assess the SCSA obtained from an auto-combustion process as pozzolanic material in blended Portland cement. SCSA was chemically and physically characterized, and its pozzolanic reactivity was assessed in pastes of hydrated lime/SCSA and Portland cement/SCSA. Finally, the compressive strength of mortars with Portland cement/SCSA proportions of 100:0, 85:15, 80:20, 75:25, and 70:30 by mass was evaluated for several curing times.

2. Materials and methods

2.1. Materials

Sugar cane straw was obtained from sugar cane plantations near the city of Ilha Solteira (São Paulo, Brazil) and was burned in a furnace by auto-combustion without temperature control for 6 h. The maximum temperature reached in the furnace was 700 °C, which is very appropriate for removing organic matter and stabilizing the amorphous phases of the SCSA. Afterwards, the SCSA obtained was passed through sieves to remove some unburned material, and the fraction that passed through was milled for 50 min to reduce the particle size in order to increase pozzolanic activity [24]. After these procedures, SCSA was characterized and assessed in pastes and mortars.

The hydrated lime ($\text{Ca}(\text{OH})_2$) used had high purity (>95% calcium hydroxide) and was mixed into pastes with SCSA in order to evaluate the pozzolanic reactivity. The Portland cement used in pastes and mortars was the Brazilian Portland Cement CPV ARI, which is composed of more than 95% clinker and does not contain pozzolans (which is appropriate for avoiding interference with the pozzolanic reaction of SCSA). Siliceous sand was obtained from Castilho city (São Paulo, Brazil) and presents a fineness modulus of 2.05 and specific gravity of 2667 kg/m³.

2.2. Methods

2.2.1. Chemical and physical characterization of SCSA

The chemical composition of SCSA was obtained through X-ray fluorescence (XRF) by means of a Philips Magix Pro XRF instrument. This test was performed to evaluate the percentages of SiO_2 and Al_2O_3 , which are important oxides in the pozzolanic reactivity [4]. To assess the mineralogical properties of the SCSA, an XRD test was carried out. The equipment used was a Seifert TT X-ray diffractometer, using $\text{Cu-K}\alpha$ radiation and a Ni filter, with a voltage of 40 kV and current intensity of 20 mA. The test was performed in the 2θ range of 5–60° with a step of 0.02° and step time of 2 s/step. The particle size of SCSA before and after milling was obtained by means of a Malvern Instruments Mastersizer 2000: the mean particle diameter (D_{med}) and median particle diameter (D_{50}) were measured to evaluate the efficiency of the milling process. SEM micrographs were taken by a JEOL JSM-6300 scanning electron microscope.

2.2.2. Preparation and characterization of hydrated lime/SCSA and Portland cement/SCSA pastes

Hydrated lime/SCSA pastes (CH/SCSA) were prepared using a hydrated lime:pozzolan:water ratio of 3:7:8 (by mass) and cured at 20 °C with a relative humidity (RH) higher than 95%. In Portland cement/SCSA mixtures (OPC/SCSA), a water/cementitious material proportion of 0.5 was selected (with the cementitious material being the sum of OPC and SCSA), and the proportions of OPC/SCSA assessed were 100/0 (control) and 85/15, and were also both cured at 20° with RH higher than 95%.

The microstructure of pastes was characterized by three instrumental techniques: Fourier transform infrared spectroscopy (FTIR, Bruker TENSOR 27 model, wavenumber spectrum between 4000 and 400 cm^{-1}), SEM (JEOL JSM-6300), and TGA (Mettler-Toledo TGA 850 model). Thermogravimetric tests were performed in 100 μL sealed pin-holed aluminum crucibles at a heating rate of 10 $^{\circ}\text{C min}^{-1}$, from 35 to 600 $^{\circ}\text{C}$, in an N_2 atmosphere (75 mL min^{-1} gas flow).

Both type of paste systems, CH/SCSA and OPC/SCSA, were analyzed by FTIR and TGA after 3, 7, 28, and 90 days of curing and by SEM after 28 days of curing. For preparation of samples for FTIR analysis and TGA, pastes were ground with acetone, filtered, and put in a laboratory oven at 60 $^{\circ}\text{C}$ for 30 min. In sample preparation for SEM analysis, small fractured pieces of paste were submerged in acetone for 1 h and put in a laboratory oven at 60 $^{\circ}\text{C}$ for 30 min.

2.2.3. Compressive strength of mortars

Compressive strengths of the mortars were measured using an EMIC Universal Machine with a 2000 kN load limit. For this test, prismatic specimens of 40 \times 40 \times 160 mm^3 were molded. Before the compressive strength measurement, three specimens were each broken in flexural mode to obtain two halves. The compressive strength was an average of six values. The proportion of water/cementitious material was 0.50, and the ratio of cementitious material to sand was 1:2.5. The replacement of Portland cement by SCSA was 0% (control), 15%, 20%, 25%, and 30% by mass. Specimens were cured at 25 $^{\circ}\text{C}$ with RH higher than 95% until the compressive strength test, which was performed after 3, 7, 28, and 90 days of curing.

3. Results and discussion

3.1. Chemical and physical characterization of SCSA

The chemical composition of SCSA measured by XRF is shown in Table 1. The material presents a low quantity of silicon dioxide (SiO_2 , 36.5%) compared with traditional siliceous pozzolans (e.g. silica fume or RHA). The presence of calcium oxide is noticeable (CaO, 16.4%), but SCSA does not have hydraulic characteristics: a mixture of this ash with alkaline medium did not harden after 24 h. The third element by percentage is potassium (expressed as K_2O , 7.9%), which is typical of some ashes from biomass [42]. Others significant compounds, such as Al_2O_3 , Fe_2O_3 , MgO, SO_3 , and P_2O_5 , are also present. A considerable loss on ignition (LOI) value (15.5%) was obtained, which was attributed to the presence of organic matter and/or carbon of unburned sugar cane straw. Thus, TGA and differential thermal analysis of SCSA showed that the main mass loss was produced in the range of 250–625 $^{\circ}\text{C}$; these are the typical volatilization/oxidation temperatures of organic matter and carbon [43]. A small mass loss was observed above 650 $^{\circ}\text{C}$ (0.34%), indicating that the presence of calcium carbonate was very low.

The XRD pattern of SCSA is shown in Fig. 1. It presented a deviation from the baseline between $2\theta = 15^{\circ}$ and $2\theta = 35^{\circ}$, which is characteristic of amorphous material. In addition, quartz (SiO_2 , PDF Card #331161), calcite (CaCO_3 , PDF Card #050586), and diopside ($\text{MgCaSi}_2\text{O}_6$, PDF Card #011-0654) were identified as impurities in the SCSA. These impurities were probably from the soil retained during the sugarcane harvesting. XRD was carried out on a sample of SCSA obtained from washed straw (without soil impurities): in this X-ray diffractogram, only some saline compounds were found, such as sylvite (KCl, PDF Card #411476), halite (NaCl, PDF Card #050628), arcanite (K_2SO_4 , PDF Card #050613), and hydroxylapatite [$\text{Ca}_5(\text{PO}_4)_3(\text{OH})$, PDF Card #090432]. These salts were formed in the calcination process from selected elements contained in the straw: sodium, chloride, potassium, calcium, sulfur, and phosphorus.

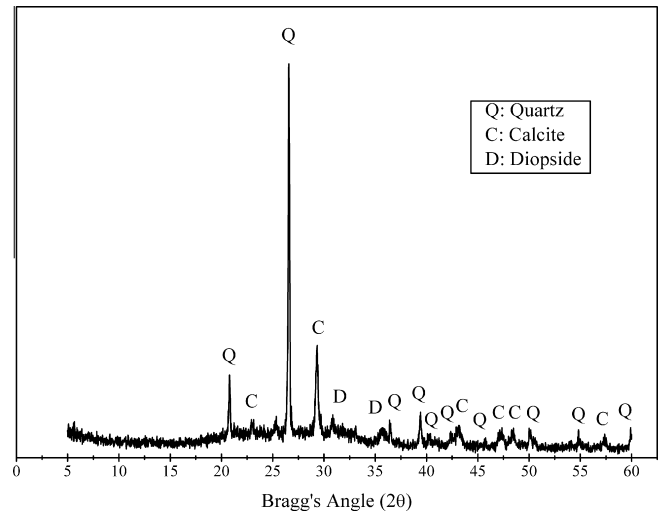


Fig. 1. X-ray diffraction pattern of SCSA.

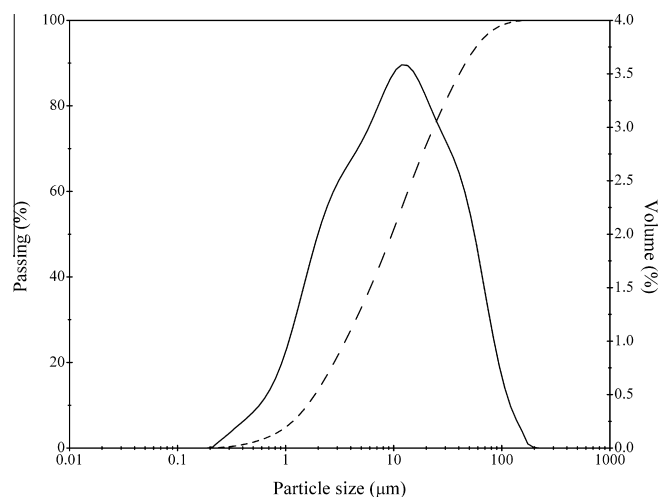


Fig. 2. Particle size distribution of SCSA (dashed line: cumulative curve; solid line: derivative curve).

The particle size distribution is shown in Fig. 2. The calculated mean particle diameter (D_{med}) of SCSA was 20.18 μm , and the median particle diameter D_{50} was 10.85 μm . Fig. 3 shows SEM micrographs for comparison of the SCSA before and after 50 min of milling. In Fig. 3a, SCSA before the milling process presents large and irregular particles, and in Fig. 3b SCSA after 50 min of milling presents smaller and more regular particles compared to SCSA without milling.

3.2. Microstructural studies of CH/SCSA pastes

CH/SCSA pastes with a 3:7 ratio, cured at 20 $^{\circ}\text{C}$, were characterized by FTIR, TGA, and SEM. FTIR spectra for hydrated lime [$\text{Ca}(\text{OH})_2$], SCSA, and CH/SCSA pastes are shown in Fig. 4. The bands of vibration for $\text{Ca}(\text{OH})_2$ are 3641 cm^{-1} (strong, O–H vibration) and

Table 1
Chemical composition of SCSA in percentage.

SiO_2	Al_2O_3	Fe_2O_3	CaO	MgO	Na_2O	K_2O	SO_3	P_2O_5	Cl	Others	LOI
36.5	2.8	3.4	16.4	7.3	0.2	7.9	4.4	4.0	0.4	1.2	15.5

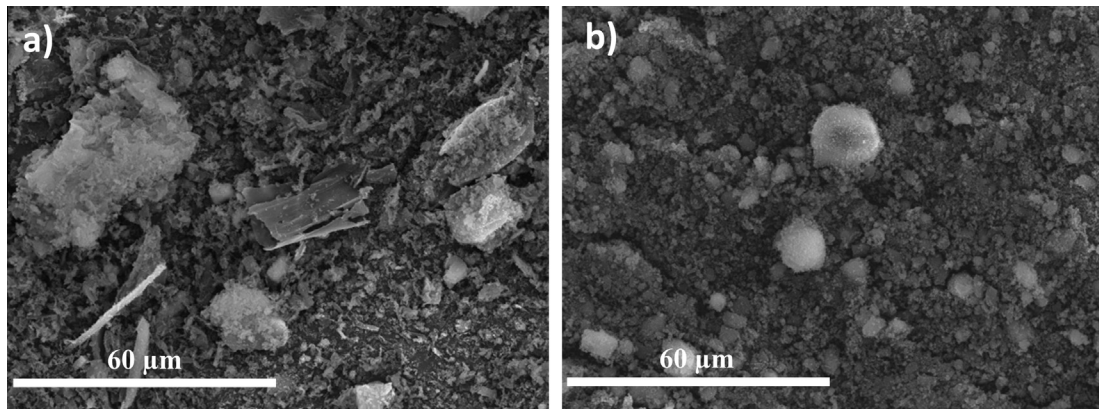


Fig. 3. SEM micrographs of SCSA: (a) before milling; (b) after 50 min of milling.

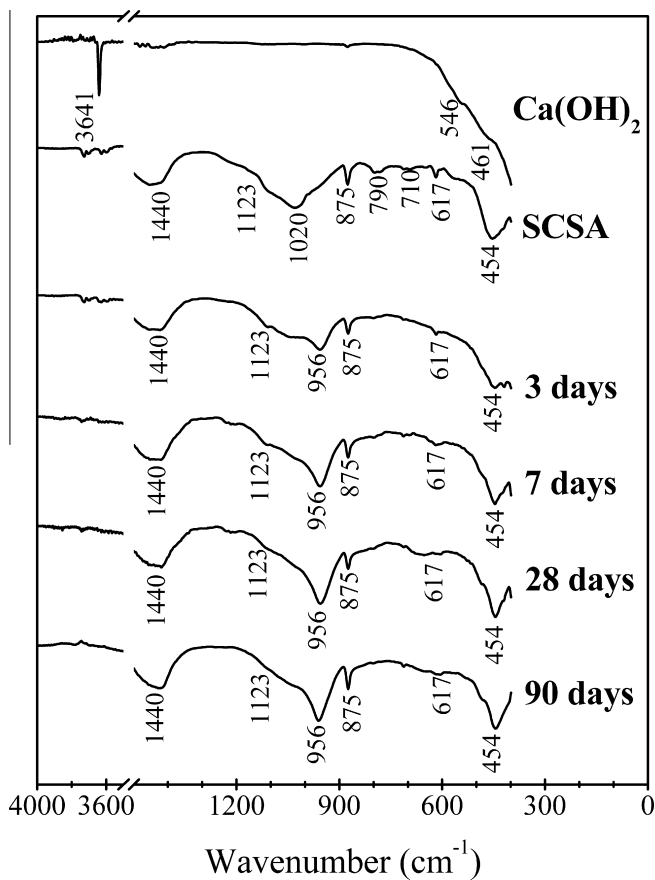


Fig. 4. FTIR spectra for CH/SCSA pastes.

there are very small peaks below 600 cm^{-1} , emphasizing the peaks at 546 and 461 cm^{-1} . For SCSA, the main vibration bands were associated with Si–O vibrations at 1123 , 1020 , 790 , 710 , 617 , and 454 cm^{-1} and with O–C–O vibrations at 1440 and 875 cm^{-1} [44].

After 3 days of curing, the main vibration bands in the paste were at 1123 , 956 , 617 , 454 (Si–O vibration), 1440 , and 875 cm^{-1} (O–C–O vibration). Firstly, it is noticed that the hydrated lime was completely reacted, because the characteristic vibration bands (at 3641 cm^{-1} and below 600 cm^{-1}) are not present in the FTIR spectrum. The vibration bands at 1123 and 454 cm^{-1} are attributed to quartz present in SCSA, because these peaks are maintained in the FTIR spectrum after the pozzolanic reaction. On the other hand, the new vibration band at 956 cm^{-1} is related to the pozzolanic

reaction products, since it was not present in the hydrated lime or in the SCSA spectra. This band can be attributed to the C–S–H gel formed in the pozzolanic reaction. Its intensity is increased with curing time, suggesting that despite the complete consumption of CH in the CH/SCSA mixture, C–S–H gel evolved with curing time, and polymerization of SiO_2 units took place. Finally, the vibration bands at 1440 and 875 cm^{-1} did not change with the pozzolanic reaction, indicating that carbonates are not involved in the process.

Derivative thermogravimetric (DTG) curves from TGA are shown in Fig. 5. Dehydration of compounds formed through pozzolanic reaction, mainly C–S–H gel, in the thermogravimetric conditions used [45], took place in the temperature range of 100 – 180°C , and the mass loss of the $\text{Ca}(\text{OH})_2$ dehydration was in the temperature range of 520 – 560°C . In this analysis, there was no mass loss at 520 – 560°C for all curing ages; that is, SCSA consumed all the $\text{Ca}(\text{OH})_2$ present in the paste. This result matches the FTIR analysis.

Table 2 summarizes the mass loss related to the dehydration of compounds from the pozzolanic reaction (P_{PZ}), $\text{Ca}(\text{OH})_2$ dehydration (P_{CH}), and lime fixation for all curing ages of CH/SCSA pastes. Since there was no peak in the DTG curves at 520 – 560°C , 100% lime fixation was achieved; that is, the SCSA consumed all the $\text{Ca}(\text{OH})_2$ added to the paste. The mass loss related to the compounds formed through the pozzolanic reaction increased with curing time due to the change in composition of these compounds:

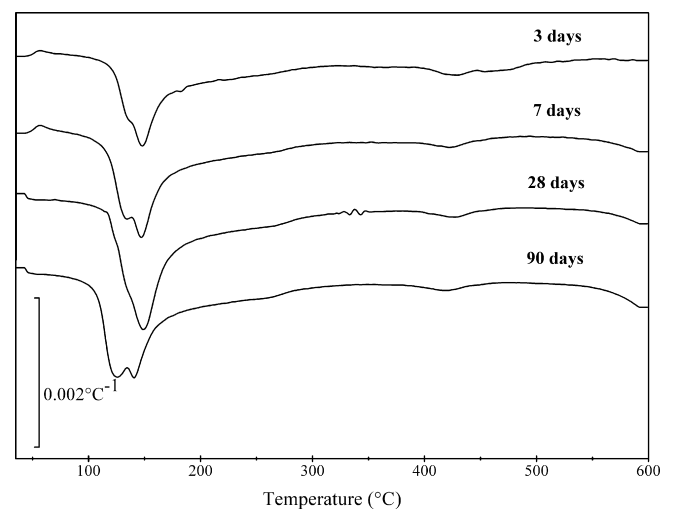


Fig. 5. DTG curves for CH/SCSA pastes.

Table 2

Mass loss of dehydration of compounds from pozzolanic reaction (P_{PZ}), from $\text{Ca}(\text{OH})_2$ dehydration (P_{CH}) and lime fixation.

Curing time (days)	P_{PZ} (%)	P_{CH} (%)	Lime fixation (%)
3	13.42	0	100
7	15.34	0	100
28	17.00	0	100
90	17.54	0	100

the C–S–H gel [with the typical formula $(\text{CaO})_x(\text{SiO}_2)_y(\text{H}_2\text{O})_n$] that initially formed had a high Ca/Si ratio (x/y). With curing time, the x/y ratio diminishes because more silica from SCSA reacts and is bonded to C–S–H gel [45]. Thus, the amount of C–S–H gel increases and then the amount of water released on heating becomes greater.

Fig. 6 shows SEM micrographs from CH/SCSA paste after 28 days of curing. As expected, taking into account TGA and FTIR assessments, an amorphous gel is formed due to the pozzolanic reaction, a dense structure is obtained, and the presence of hydrated lime is not noticed. Some C–S–H gel appeared in the form of needle-like products.

3.3. Microstructural studies of OPC/SCSA pastes

OPC/SCSA pastes with an 85:15 ratio, cured at 20 °C, were characterized by FTIR, TGA, and SEM. Also, control OPC pastes were prepared for comparison. Fig. 7 shows the FTIR spectra for anhydrous OPC, SCSA, OPC pastes, and OPC/SCSA pastes. The vibration bands for unhydrated OPC related to Si–O vibrations are at 933, 873, 519, and 449 cm^{-1} . After 3 days of curing, the OPC pastes showed a main Si–O type vibration band at 956 cm^{-1} (due to the Si–O stretching in polymeric SiO_4 units produced in the hydration of calcium silicates), and another two O–C–O bands were observed at 1420 and 873 cm^{-1} . The paste containing SCSA also presented a peak at 1123 cm^{-1} (Si–O vibration), which was also found in the original SCSA. Firstly, it is noticed that the vibration band at 956 cm^{-1} of OPC/SCSA pastes is similar to those found in CH/SCSA pastes (Fig. 4), which means the products of the pozzolanic reaction (C–S–H gel) are similar to those obtained by the OPC hydration. The broadness of this main vibration band for the OPC/SCSA hydrated sample was due to the SCSA (the ash presented a band at 1020 cm^{-1}), indicating that this material reacted completely in the conditions of the hydration of cement. Finally, the vibration band at 1123 cm^{-1} (which did not appear in OPC paste) is related to the quartz present in SCSA; this mineral did not react in the studied conditions. After 7, 28, and 90 days of curing, pastes did not

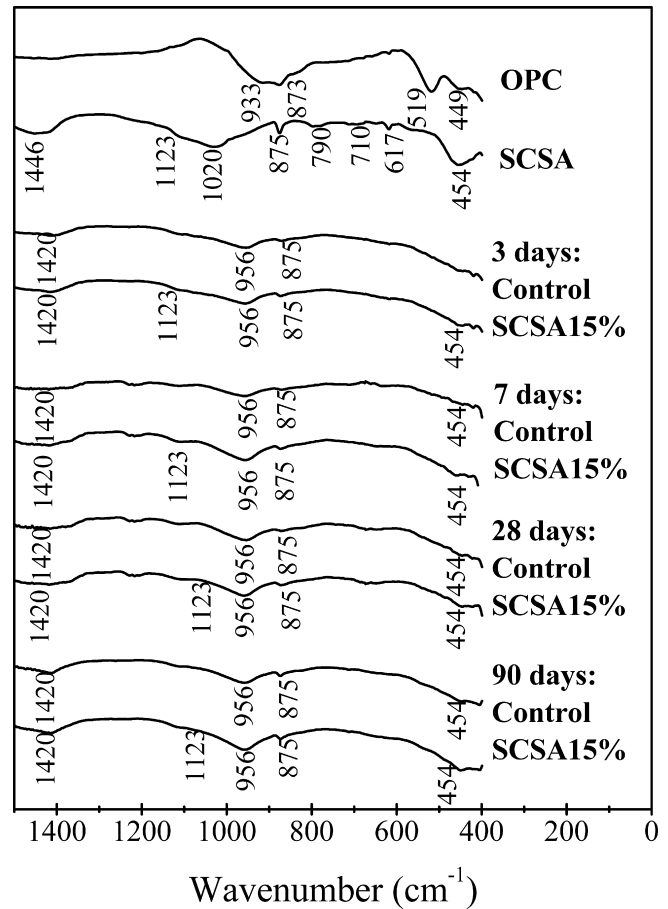


Fig. 7. FTIR spectra for anhydrous OPC, SCSA, OPC pastes, and OPC/SCSA pastes.

show significant changes compared to 3 days of curing; it may be noticed that the band intensity increased for the 956 cm^{-1} signal (related to the higher amount of C–S–H gel). The diminution of its shoulder at higher wavenumbers in OPC/SCSA pastes suggested the reaction of SCSA and the dissolution/transformation of this material due to the pozzolanic process.

DTG curves for OPC/SCSA pastes are shown in Fig. 8. Similar hydration products were found for both OPC and OPC/SCSA pastes. For all curing times, the peak present at 550 °C is smaller in the SCSA-containing paste compared to the control. This behavior is due to two effects: on one hand, the dilution effect when SCSA

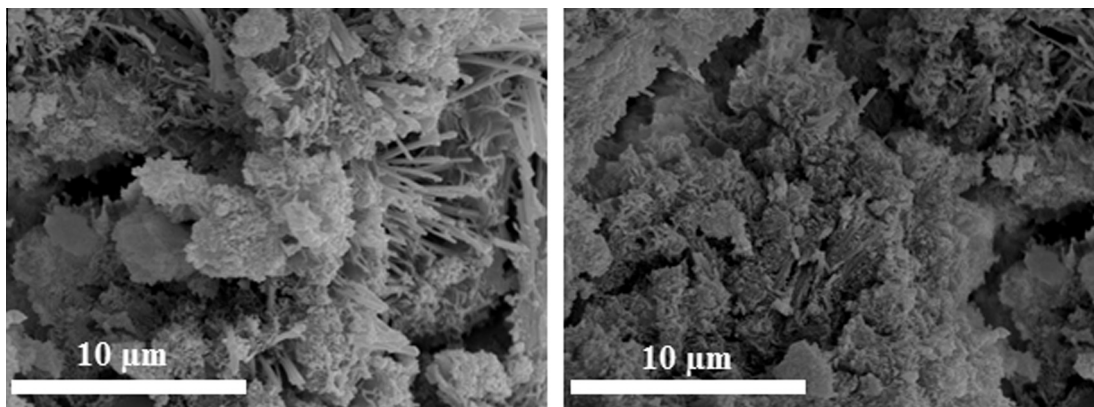


Fig. 6. SEM images of CH/SCSA paste after 28 days of curing.

Table 3

Mass loss in the dehydration of compounds from OPC/pozzolanic reaction ($P_{\text{OPC+PZ}}$), $\text{Ca}(\text{OH})_2$ dehydration (P_{CH}) and lime fixation for OPC and OPC/SCSA (15% replacement) pastes.

Curing time (days)	$P_{\text{OPC+PZ}}$ (%)		P_{CH} (%)		Lime fixation (%)
	OPC	OPC/SCSA	OPC	OPC/SCSA	
3	13.79	15.09	2.40	1.64	19.61
7	15.47	16.00	2.51	1.68	21.26
28	17.43	17.36	2.92	1.53	38.36
90	17.53	17.49	3.20	1.60	41.18

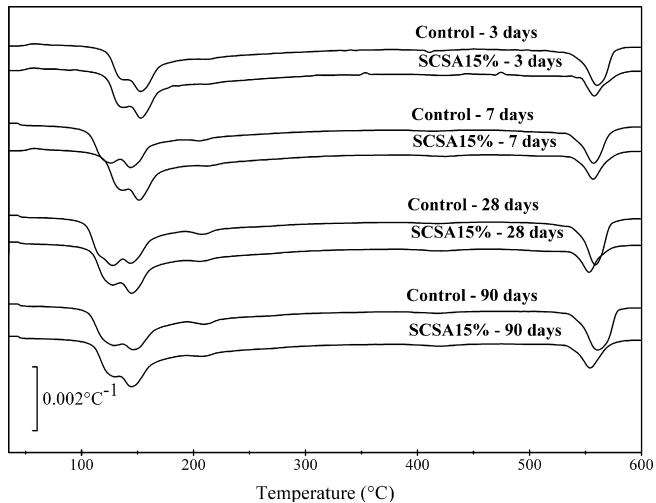


Fig. 8. DTG curves for OPC and OPC/SCSA (15% replacement) pastes for different curing times.

replaced OPC, because less portlandite was formed in the hydration of cement, and on the other hand, the consumption of the portlandite by reaction towards SCSA.

Mass loss related to the dehydration of compounds from OPC and the pozzolanic reaction ($P_{\text{OPC+PZ}}$), $\text{Ca}(\text{OH})_2$ dehydration (P_{CH}), and lime fixation for OPC and OPC/SCSA pastes at all curing ages are summarized in Table 3. It is noticed that the $P_{\text{OPC+PZ}}$ value increases with curing age for both pastes, but the paste with SCSA presents higher values compared to the control at the earliest curing times (3 and 7 days). This behavior showed that the pozzolanic material is very reactive. Additionally, the SCSA particles present act as nucleation sites for hydration products from OPC,

Table 4

Compressive strength of mortar values (MPa) and their standard deviation.

Specimen/curing age	3 days	7 days	28 days	90 days
Control	32.93 ± 1.13	36.06 ± 1.94	41.56 ± 1.70	44.01 ± 2.25
SCSA15%	32.27 ± 1.30	34.53 ± 0.12	40.55 ± 1.27	44.33 ± 2.55
SCSA20%	31.08 ± 1.41	36.56 ± 1.11	42.82 ± 1.41	44.42 ± 2.38
SCSA25%	30.55 ± 0.98	33.97 ± 1.87	42.51 ± 1.51	43.99 ± 1.82
SCSA30%	31.83 ± 0.16	34.73 ± 0.56	40.28 ± 1.41	40.99 ± 1.11

enhancing the hydration reaction rate. This reactivity was quantified by means of lime fixation. After 3 days of curing, 19.61% of the portlandite released in the hydration of OPC in OPC/SCSA paste was consumed; this behavior indicated that the pozzolanic reactivity was important at earlier curing ages. The pozzolanic reactivity increased with curing time, and the percentage lime fixation reached 41.18% after 90 days.

Fig. 9 shows SEM micrographs of OPC and OPC/SCSA pastes. In both figures, there is a dense and amorphous structure, but the control OPC paste (Fig. 9a) presents more portlandite compared to the OPC/SCSA paste (Fig. 9b). This is in agreement with the thermogravimetric results.

3.4. Compressive strength of mortars

Five sets of mortars were prepared: control mortar (only OPC as cementitious compound) and four mortars in which 15–30% of the OPC by mass was replaced by SCSA. The SCSA mortar nomenclature is SCSAXX%, where XX is the percentage replacement (15, 20, 25, or 30%). Values of the mortars' compressive strengths and their standard deviations are listed in Table 4. All mortars showed a continuous increase in the compressive strength with curing time as expected. Interestingly, after 3 days of curing, all mortars containing SCSA presented compressive strength values very similar to that obtained for the control mortar. This is related to the high reactivity of the ash, which agrees with the behavior described in the paste studies. This trend was also observed for curing periods of 7–90 days. In this case, the consumption of portlandite by SCSA (observed by TGA) for longer curing times did not lead to evidence of enhancement in the development of compressive strength.

In general terms, from the point of view of strength development, and taking into account the important replacement levels achieved in this study, it can be established that the SCSA-containing mortars show an important strength gain.

Fig. 10 shows the compressive strength gain (SG) [46] of SCSA mortars. This SG was calculated taking into account the percentage

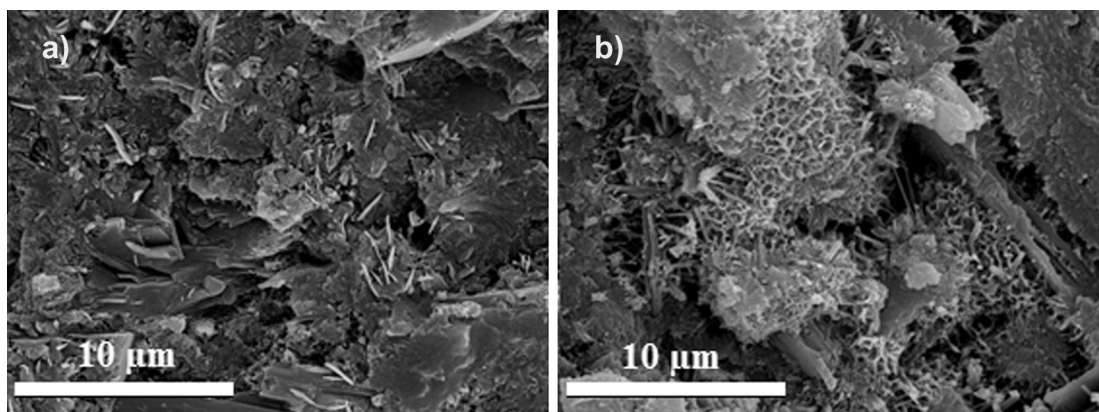


Fig. 9. SEM images of pastes after 28 days of curing: (a) control OPC; (b) OPC/SCSA (15% replacement).

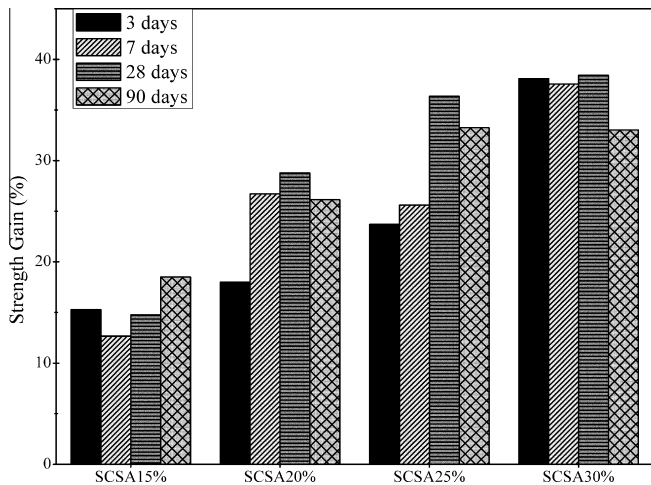


Fig. 10. Strength gain (SG) for SCSA-containing mortar at 3, 7, 28, and 90 days of curing.

replacement of OPC by pozzolan; the compressive strength of OPC/SCSA mortar (R_i) was compared with the strength of the OPC mortar (R_o), which was corrected by means of the ratio between OPC mass (w_{cem}) and the binder mass (sum of OPC and pozzolan, $w_{cem} + w_{puz}$). In this case, relative values were calculated as percentages as follows:

$$SG = \frac{R_i - \left[R_o * \frac{w_{cem}}{w_{cem} + w_{puz}} \right]}{\left[R_o * \frac{w_{cem}}{w_{cem} + w_{puz}} \right]} * 100 \quad (1)$$

All SG values calculated according to Eq. (1) were positive values, indicating the high effectiveness of SCSA in cement mixtures. Calculated SG values are depicted in Fig. 10. SG values increased with the percentage replacement.

In general, there are similar SG values for different curing ages with the same SCSA replacement, indicating the high activity of the pozzolanic material. These results show that the SCSA can replace the Portland cement up to high percentages.

4. Conclusions

SCSA was chemically and physically characterized. The material presented a relatively low content of SiO_2 (36%) and high unburned fraction (LOI = 15.5%). A baseline deviation in XRD results between 15° and 35° showed the presence of amorphous fraction, which was probably reactive from the pozzolanic point of view. Pozzolanic reactivity was confirmed by means of thermogravimetric studies on hydrated lime and ordinary Portland cement pastes.

In hydrated lime/SCSA pastes, TGA showed that pozzolanic material completely consumed the available calcium hydroxide after 3 days of curing. When 15% of the cement paste was replaced by SCSA, more than 40% of the portlandite was fixed, and SEM images showed a lower presence of portlandite crystals.

Finally, from the study of mortars, SCSA presented an important contribution to the development of compressive strength when 15–30% of Portland cement by weight was replaced. Pozzolanic activity was observed after 3 days of curing, and all mortars showed compressive strength close to that of the control for all curing ages. In the strength gain analysis, the highest replacements (25% and 30%) presented similar results after 28 and 90 days of curing, indicating that SCSA can be used as a pozzolanic admixture for high replacement levels in blended mortars.

Acknowledgements

The authors would like to thank CNPq-Brazil (process n° 401724/2013-1) and the Ministerio de Educación, Cultura y Deporte of Spain (the Cooperación Interuniversitaria program with Brazil: PHB-2011-0016-PC). We also thank CAPES-Brazil for the Grant for J.C.B. Moraes and Electron Microscopy Service of the Universitat Politècnica de València.

References

- [1] FICEM (Inter-American Cement Federation). Statistical Report 2013. <http://www.ficem.org/estadisticas/statistical_report_2013.pdf>. (11 Mar 2014).
- [2] J.H. Sharp, E.M. Gartner, D.E. Macphee, Novel cement system (sustainability). Session 2 of the Fred Glasser Cement Science Symposium, *Adv. Cem. Res.* 22 (4) (2010) 195–202.
- [3] X. Guo, H. Shi, W.A. Dick, Compressive strength and microstructural characteristics of class C fly ash geopolymer, *Cem. Concr. Compos.* 32 (2010) 142–147.
- [4] P.C. Hewlett, *Lea's chemistry of cement and concrete*, 4th ed., Elsevier, 2008.
- [5] E. Vejmelková, M. Keppert, P. Rovnaníková, Z. Keršner, R. Cerný, Application of burnt clay shale as pozzolan addition to lime mortar, *Cem. Concr. Compos.* 34 (2012) 486–492.
- [6] S. Sánchez-Moral, L. Luque, J.C. Cañaveras, V. Soler, J. García-Guinea, A. Aparicio, Lime pozzolana mortars in Roman catacombs: composition, structures and restoration, *Cem. Concr. Res.* 35 (2004) 1555–1565.
- [7] M. Ghrici, S. Kenai, E. Meziane, Mechanical and durability properties of cement mortar with Algerian natural pozzolana, *J. Mater. Sci.* 41 (2006) 6965–6972.
- [8] A.A. Ramezaniapur, H.B. Jovein, Influence of metakaolin as supplementary cementing material on strength and durability of concretes, *Constr. Build. Mater.* 30 (2012) 470–479.
- [9] S. Abd-El-Aleem, M.A. Abd-El-Aziz, H. El-Didamony, Calcined carbonaceous shale pozzolanic Portland cement, *Egypt. J. Chem.* 45 (3) (2002) 501–517.
- [10] H. El-Didamony, S. Abd-El-Aleem, Calcination and hydration characteristics of carbonaceous shale – limestone mixes, *Sil. Ind.* 67 (11–12) (2002) 123–128.
- [11] Y. Senhadji, G. Escadeillas, M. Mouli, H. Khelafi, Benosman, Influence of natural pozzolan, silica fume and limestone fine on strength, acid resistance and microstructure of mortar, *Powder Technol.* 254 (2014) 314–323.
- [12] E. Ghiasvand, A.A. Ramezaniapur, A.M. Ramezaniapur, Effect of grinding method and particle size distribution on the properties of Portland-pozzolan cement, *Constr. Build. Mater.* 53 (2014) 547–554.
- [13] K. Celik, C. Meral, M. Mancio, P.K. Mehta, P.J.M. Monteiro, A comparative study of self-consolidating concretes incorporating high-volume natural pozzolan or high-volume fly ash, *Constr. Build. Mater.* 67 (2014) 14–19.
- [14] G. Peng, Q. Ma, H. Hu, R. Gao, Q. Yao, Y. Liu, The effects of air entrainment and pozzolans on frost resistance of 50–60 MPa grade concrete, *Constr. Build. Mater.* 21 (2007) 1034–1039.
- [15] N. Kaid, M. Cyr, S. Julien, H. Khelafi, Durability of concrete containing a natural pozzolan as defined by a performance-based approach, *Constr. Build. Mater.* 23 (2009) 3457–3467.
- [16] M. Nili, A.M. Salehi, Assessing the effectiveness of pozzolans in massive high-strength concrete, *Constr. Build. Mater.* 24 (2010) 2108–2116.
- [17] V. Sata, C. Jaturapitakkul, K. Kiattikomol, Influence of pozzolan from various by-product materials on mechanical properties of high-strength concrete, *Constr. Build. Mater.* 21 (2007) 1589–1598.
- [18] V.T. Giner, S. Ivorra, F.J. Baeza, E. Zornoza, B. Ferrer, Silica fume admixture effect on the dynamic properties of concrete, *Constr. Build. Mater.* 25 (2011) 3272–3277.
- [19] G. Belén, M. Fernando, M. Isabel, E. Javier, Structural shear behaviour of recycled concrete with silica fume, *Constr. Build. Mater.* 23 (2009) 3406–3410.
- [20] S.W.M. Supit, F.U.A. Shaikh, P.K. Sarker, Effect of ultrafine fly ash on mechanical properties of high volume fly ash mortar, *Constr. Build. Mater.* 51 (2014) 278–286.
- [21] J. Payá, J. Monzó, M.V. Borrachero, Outstanding aspects on the use of rice husk ash and similar agrowastes in the preparation of binders, in: *Proc First Pro-Africa Conf: Non conventional building materials based on agroindustrial wastes*. Pirassununga, 18–19 Oct 2010, São Paulo, Brazil.
- [22] P. Asha, A. Salman, R.A. Kumar, Experimental study on concrete with bamboo leaf ash, *Int. J. Eng. Adv. Technol.* 3 (2014) 46–51.
- [23] J. Payá, J. Monzó, M.V. Borrachero, E. Peris-Mora, L.M. Ordóñez, Studies on crystalline rice husk ashes and the activation of their pozzolanic properties, *Waste Manage.* 1 (2000) 493–503.
- [24] G.C. Cordeiro, R.D. Toledo Filho, L.M. Tavares, E.M.R. Fairbairn, Ultrafine grinding of sugar cane bagasse ash for application as pozzolanic admixture in concrete, *Cem. Concr. Res.* 39 (2009) 110–115.
- [25] G.C. Cordeiro, R.D. Toledo Filho, E.M.R. Fairbairn, Effect of calcination temperature on the pozzolanic activity of sugar cane bagasse ash, *Constr. Build. Mater.* 23 (2009) 3301–3303.
- [26] E. Aprianti, P. Shafiq, S. Bahri, J.N. Farahani, Supplementary cementitious materials origin from agricultural wastes – a review, *Constr. Build. Mater.* 74 (2015) 176–187.
- [27] S. Demis, J.G. Tapali, V.G. Papadakis, An investigation of the effectiveness of the utilization of biomass ashes as pozzolanic materials, *Constr. Build. Mater.* 68 (2014) 291–300.

- [28] UNICA (União da Indústria de Cana-de-Açúcar). Produção de cana-de-açúcar, 2003/2014 – 2013/2014. <<http://www.unicadata.com.br>>. Accessed 18 Sept 2014.
- [29] S.M. Costa, P.G. Mazzola, J.C.A.R. Silva, R. Pahl, A. Pessoa Jr., S.A. Costa, Use of sugar cane straw as a source of cellulose for textile fiber production, *Ind. Crop Prod.* 42 (2013) 189–194.
- [30] BNDES and CGEE (Centro de Gestão e Estudos Estratégicos). Sugarcane-based bioethanol: energy for sustainable development. 1st ed. Rio de Janeiro, Brazil; 2008.
- [31] M.L.C. Ripoli, C.A. Gamero, Palhiço de cana-de-açúcar: ensaio padronizado de recolhimento por enfiamento cilíndrico, *Energia na Agricultura (Brazil)* 22 (1) (2007) 75–93.
- [32] L.W.S. Hoi, B.S. Martincigh, Sugar cane plant fibres: separation and characterization, *Ind. Crop Prod.* 47 (2013) 1–12.
- [33] K. Deepchand, Characteristics, present use and potential of sugar cane tops and leaves, *Agric. Wastes* 15 (1986) 139–148.
- [34] E. Hugot, *Handbook of cane sugar engineering*, 3rd ed., Elsevier Science, Amsterdam, 1986.
- [35] M. Frías, E. Villar-Cociña, E. Valencia-Moraes, Characterization of sugar cane straw waste as pozzolanic material for construction: calcining temperature and kinetic parameters, *Waste Manage.* 27 (2007) 533–538.
- [36] J.F. Martirena, B. Middendorf, M. Gehrke, H. Budelmann, Use of wastes of the sugar industry as pozzolana in lime-pozzolana binders: study of the reaction, *Cem. Concr. Res.* 28 (11) (1998) 1525–1536.
- [37] E. Villar-Cociña, E.V. Moraes, R.G. Rodríguez, J.H. Ruíns, Kinetics of the pozzolanic reaction between lime and sugar cane straw ash by electrical conductivity measurement: a kinetic-diffusive model, *Cem. Concr. Res.* 33 (2003) 517–524.
- [38] J.F. Martirena, B. Middendorf, R.L. Day, M. Gehrke, P. Roque, L. Martínez, S. Betancourt, Rudimentary, low tech incinerators as a means to produce reactive pozzolan out of sugar cane straw, *Cem. Concr. Res.* 36 (1998) 1056–1061.
- [39] A. Guzmán, C. Gutiérrez, V. Amigó, R. Mejía de Gutiérrez, S. Delvasto, Pozzolanic evaluation of the sugar cane leaf, *Mater. Constr.* 61 (2011) 213–225.
- [40] E.V. Moraes, E. Villar-Cociña, M. Frías, S.F. Santos, H. Savastano Jr., Effects of calcining conditions on the microstructure of sugar cane waste ashes (SCWA): Influence in the pozzolanic activation, *Cem. Concr. Comp.* 31 (2009) 22–28.
- [41] E. Villar-Cociña, M. Frías, E.V. Moraes, M.I.S. Rojas, An evaluation of different kinetic models for determining the kinetic coefficients in sugar cane straw-clay ash/lime system, *Adv. Cem. Res.* 18 (1) (2006) 17–26.
- [42] S. Demis, J.G. Tapali, V.G. Papadakis, An investigation of the effectiveness of the utilization of biomass ashes as pozzolanic materials, *Constr. Build. Mater.* 68 (2014) 291–300.
- [43] J. Payá, J. Monzó, M.V. Borrachero, L. Díaz-Pinzón, L.M. Ordóñez, Sugar-cane bagasse ash (SCBA): studies on its properties for reusing in concrete production, *J. Chem. Technol. Biotechnol.* 77 (2002) 321–325.
- [44] A. Allahverdi, B. Shaverdi, E. Kani, Influence of sodium oxide on properties of fresh and hardened paste of alkali-activated blast-furnace slag, *Int. J. Civ. Eng.* 8 (2010) 304–314.
- [45] C.L. Pereira, H. Savastano Jr., J. Payá, S.F. Santos, M.V. Borrachero, J. Monzó, Use of highly reactive rice husk ash in the production of cement matrix reinforced with green coconut fiber, *Ind. Crop Prod.* 49 (2013) 88–96.
- [46] J. Payá, J. Monzó, M.V. Borrachero, Physical, chemical and mechanical properties of fluid catalytic cracking catalyst residue (FC3R) blended cements, *Cem. Concr. Res.* 31 (2001) 57–61.